Supporting Information for:

Measurements of Entangled Two-Photon Absorption in Organic Molecules with CW Pumped Type-I Spontaneous Parametric Down-Conversion

Juan P. Villabona-Monsalve†, Ryan K. Burdick†, Theodore Goodson III†*

†Department of Chemistry, University of Michigan, Ann Arbor, MI 48109

*tgoodson@umich.edu

1) *Absorption spectra*

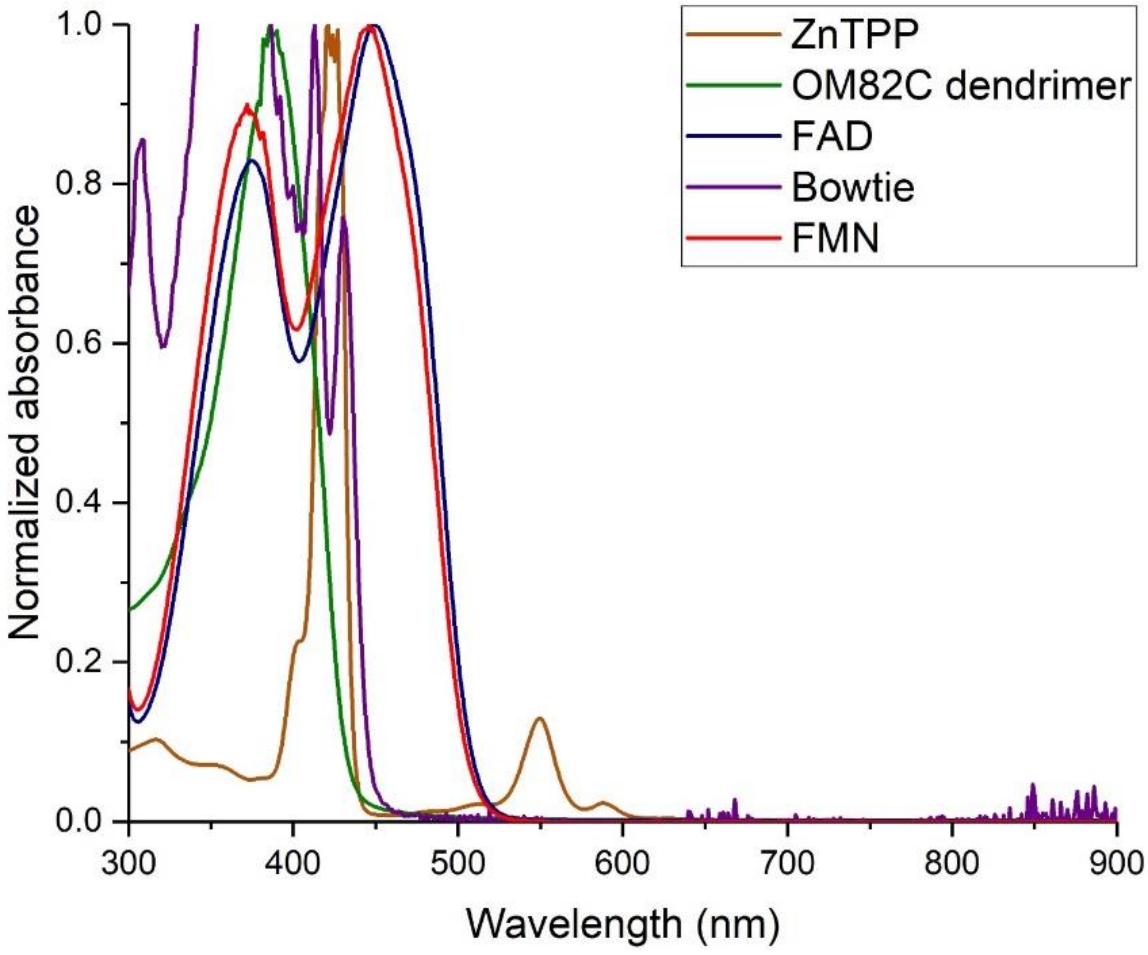

Figure S1. Absorption spectra of all molecules studied in this work.

2) ***Joint frequency spectrum and Schmidt decomposition***

To calculate *K* and *E* of the SPDC photons in our experiment, the joint photon frequency spectrum must be measured, and then the Schmidt decomposition performed on this spectrum. First, the entangled photons are passed through a bandpass (BP) filter centered at the degenerate wavelength (810 nm) so that only wavelengths within the APD's detection range are collected. The photons are then separated from each other in space. For non-collinear phase-matching, the entangled photons can easily be separated from each other with a mirrored knife-edge prism. Once separated, each photon is sent through its monochromator and focused onto its APD. The joint frequency spectrum is measured by performing a series of scans as follows: one monochromator (Bob's) for the signal photon is set at a given wavelength (e.g. 840 nm). Then the other monochromator (Alice's) for the idler photon is scanned across the wavelength range of the bandpass filter (775-845 nm in our experiment). Photon counts after the two monochromators are measured in coincidence. The sum of the entangled photons' frequencies must equal the pump photon's frequency: $\omega_A + \omega_B = \omega_p$, or equivalently, $\frac{1}{\lambda_A} + \frac{1}{\lambda_B} = \frac{1}{\lambda_p}$. Additionally, two entangled photons are also strongly correlated in time, so they can only produce a coincidence count with each other. Therefore, if Alice's photon is entangled with Bob's 840 nm photon, coincidence counts should be registered when, and only when, Alice has her monochromator set at 780 nm. The joint frequency spectrum is obtained by scanning one of the monochromators, while the other´s wavelength is kept fixed.

There is a very small chance that two photons that are not entangled happen to arrive at the two APDs within the coincidence window, known as an accidental count. These accidental counts can be subtracted out of the true coincidence count signal. They can be measured by adding a delay to one of the APD's channels to the coincidence counter. This delay (100 ns in our experiment) must be longer than the coincidence window (10 ns in our experiment) so that only the accidental coincidence counts are measured and can then be subtracted from the joint frequency spectrum. The joint frequency spectrum then only contains coincidence counts from entangled photon pairs.

Before applying the Schmidt decomposition to the experimental joint frequency spectrum, we can make the decomposition more precise by fitting the experimental spectrum with an analytical model and applying the decomposition to this analytical model. The model

consists of two components: the joint photon intensity (i.e. square of the joint photon amplitude) and the BP filter used in the experiment. It has previously been shown that in the limit of long-pulse-width pumping of SPDC (of which CW pumping is the most extreme limit), the joint photon amplitude of Type I SPDC can be accurately modeled with a double-Gaussian[1]:

$$z = A \cdot exp\left[\begin{matrix} -\frac{1}{2}\left(\frac{x\cdot cos(\theta)+y\cdot sin(\theta)-x_c\cdot cos(\theta)-y_c\cdot sin(\theta)}{\omega_1}\right)^2 \\ -\frac{1}{2}\left(\frac{-x\cdot sin(\theta)+y\cdot cos(\theta)+x_c\cdot sin(\theta)-y_c\cdot cos(\theta)}{\omega_2}\right)^2 \end{matrix} \right] \quad \text{(S1)}$$

where A is the maximum coincidence count probability, x (y) is the frequency of Alice's (Bob's) photon, x_c (y_c) is the central frequency of Alice's (Bob's) one-photon amplitude, ω_1 (ω_2) is the diagonal (anti-diagonal) width of the two-photon amplitude, and θ is the angle of the coincidence count amplitude relative to the x-axis. These parameters are labeled in the example double-Gaussian contour plot in Fig. S2.

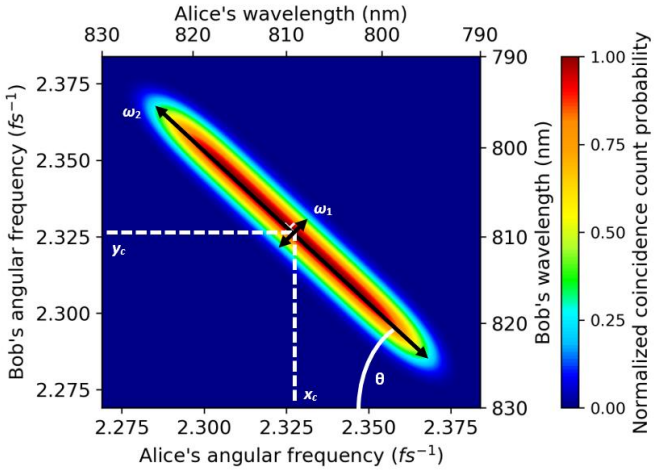

Figure S2. Example double-Gaussian showing the parameters to be optimized. Note: when normalized, $A = 1$.

The double-Gaussian model is particularly attractive because the Schmidt modes of a double-Gaussian can be found analytically[1]. Additionally, the double-Gaussian in eq. (S1) contains only real terms, which is important when one considers that in our experiment with APDs, we measure the joint photon *intensity*, not the joint photon *amplitude*. Therefore, our

experimental data must be fit with the square of the double-Gaussian in eq. (S1), and this can be completed in Matlab. Since all terms are real, we can use the square root of our fit as the absolute value of the joint photon amplitude for the Schmidt decomposition. When calculating K and E, the square of the Schmidt coefficients are used, so the use of the absolute value of the joint amplitude does not affect our calculation of K and E.

To confirm the accuracy of our model, we experimentally measured the joint frequency spectrum of SPDC filtered with a BP filter centered at 810 nm with FWHM = 30 nm (810-30 nm BP filter) and compared this experimental data with the model's calculation of the joint frequency spectrum, where the model is the double-Gaussian spectral amplitude times the 810-30 nm BP filter function. The results are shown in Fig. S3. We compared slices of the 2D model to the experimental data at various points of interest: a) when energy is conserved so that $\omega_A + \omega_B = \omega_p$, b) when Bob's wavelength is constant at the degenerate wavelength, 810 nm, and c) when $\omega_A = \omega_B$. These plots are also shown in Fig. S3. All plots and data have been normalized.

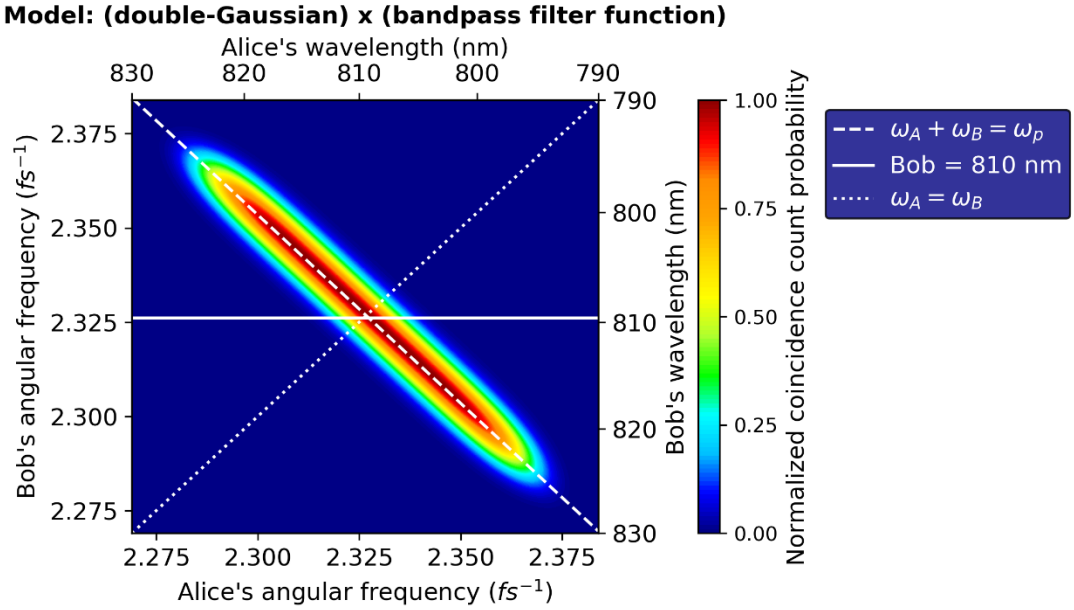

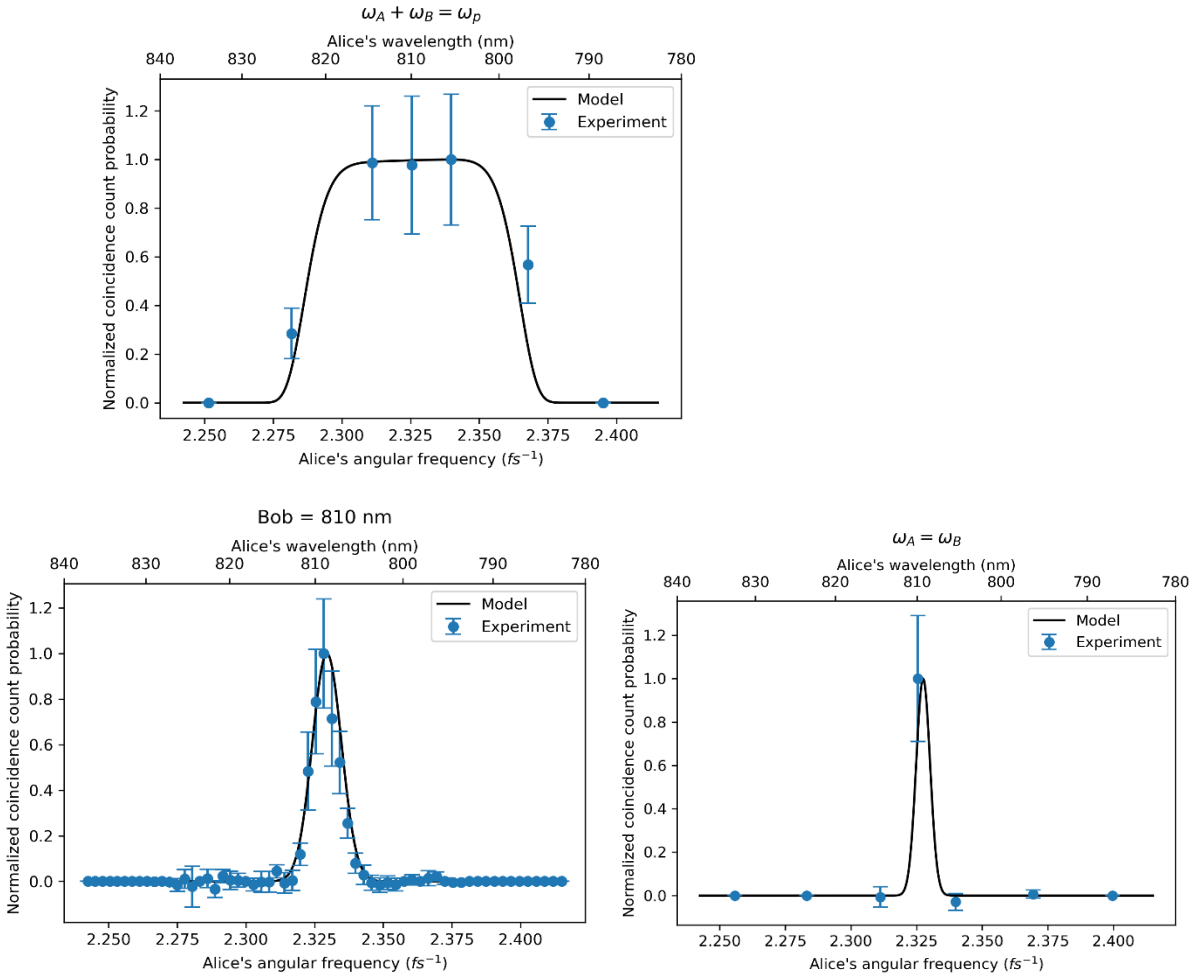

Figure S3. Model of non-collinear Type-I degenerate, CW-pumped SPDC filtered by an 810-30 nm BP filter. Shown is the full 2D model as well as slices used to compare with experimental data.

The plots in Fig. S3 confirms that our fitted model of the filtered SPDC joint frequency spectrum accurately compares to experimental data. Therefore, to quantify the degree of frequency entanglement of our filtered SPDC photons, the Schmidt decomposition is performed on this fitted model of the joint frequency spectrum. Since the Schmidt decomposition is a continuous function reformulation of the matrix formulated singular value decomposition (SVD), we can discretize our continuous function model into a matrix. The SVD can then be performed on the matrix form of our fitted model using the SVD function from a linear algebra programming package, such as NumPy or Matlab. With the calculated Schmidt coefficients, we then determine K and E, as shown in the manuscript.

3) *ETPA signal details*

Error bars are calculated as the propagated error from the standard deviation of 5 measurements. For a reference "blank," we measure the entangled photon transmission through two different pure solvent trials. The difference in their transmission is the baseline of the experiment, and we subtract that baseline from the measured ETPA signal. When removing the solvent from the cuvette and adding either the chromophore solution or second solvent sample, the black box containing the cuvette always remains closed. An injection port connecting the lid of the box to the cuvette allows for easy removal and addition of liquid from the cuvette. By not opening the box during experiments, the entangled photon alignment on the APD remains as steady as possible, which helps to lower the noise level and limit of detection of the experiment.

Analysis of potential signals interfering with the ETPA signal

The probability of OPA at the entangled photon wavelength (810 ± 15 nm) is very small since none of the chromophores have excited states near the entangled photon wavelength. Any small loss due to OPA can be estimated using the UV-vis absorbance at 810 ± 15 nm. Since there are no excited states at those wavelengths (Fig. S1), we can use the limit of detection of the spectrophotometer as an upper-bound for OPA: absorbance = ~0.0005, which equates to a 0.1 % loss in transmission. For an input of 10^6 photons/s, this loss equates to, at most, 10^3 photons/s, 1-2 orders of magnitude smaller than the chromophore's loss in transmission in our ETPA experiment. Classical TPA cross-sections of chromophores are typically around ~10^{-47} cm^4/s/molecule or smaller, which could only result in an extremely small loss in transmission of 10^{-11} photons/s.

Previous ETPA experiments have used chromophore concentrations as high as 110 mM without noticeable scattering from the chromophore.[2] To be cautious with avoiding scattering, we use solutions no more concentrated than 1 mM, where the chromophore-to-solvent molecule ratio is at most ~1:10^4. Scattering detected from such a diluted solution comes mainly from the solvent, and the solvent scattering is typically around 1-2 orders of magnitude larger than the chromophore's scattering in dilute solutions.[3] Anyway, scattering from the solvent is accounted for in the pure solvent transmission scan and is subtracted out of the ETPA signal. Nonetheless, we can estimate the intensity of scattering from both the chromophore and solvent to definitively

rule out the possibility of scattering contributing to our measured signal. For the chromophores, the most probable sources of scattering could come from non-resonant Rayleigh scattering at 810 nm or resonant hyper-Rayleigh scattering of the entangled photon pair at the two-photon energy, 405 nm. It has been shown that for chromophores with molar extinction coefficients of ~10^5 M^{-1} cm^{-1} (which is typical for chromophores, if not smaller), the intensity of resonance Rayleigh scattering is only $4x10^{-6}$ of the one-photon absorption at the same wavelength.[4] The intensity of non-resonant Rayleigh scattering would be an additional 1-2 orders of magnitude smaller than the resonance Rayleigh scattering.[3] Using our estimate of OPA at 810 ± 15 nm, the non-resonant Rayleigh scattering of the chromophore would at most be 10^{-4} photons/s. To estimate resonant hyper-Rayleigh scattering, we first estimate the non-resonant hyper-Rayleigh scattering intensity, which is 3-4 orders of magnitude smaller than non-resonant Rayleigh scattering.[5] Resonant hyper-Rayleigh scattering can have an enhancement over the non-resonant scattering by about a factor of 5.[6] Therefore, at most, the loss in transmission from resonant hyper-Rayleigh scattering would be 10^{-6} photons/s. Raman or hyper-Raman scattering would have even smaller intensities.

For the solvent, the scattering cross-section for an organic solvent is on the order of 10^{-26} cm^2/molecule.[7] We calculate the number of solvent molecules within the beam path using its density and estimate that the solvent would only scatter 10^{-2} photons/s. As expected, the solvent would scatter more than the chromophore by 2 orders of magnitude,[3] but the solvent scattering is still several orders of magnitude smaller than ETPA.

To reduce the mechanical movement of the equipment during the experiment, we use an injection port attached to the cuvette that opens at the lid of the black box containing all the optics and detectors. We can remove and refill liquid in the cuvette without opening the black box or disturbing the equipment inside it. In this way, all sources of mechanical movement in the setup are significantly reduced.

The noise level, or baseline, of our ETPA experiment, is measured by comparing the entangled photon transmission for two different pure solvent trials. The process of removing the first solvent trial from the cuvette and replacing it with the second solvent trial in the cuvette perfectly mimics the process of adding a chromophore solution to the cuvette. This process accounts for any remaining movement to the equipment caused by inserting the pipette into the injection port. It also accounts for fluctuations in the average pump laser power over time, which would change the input entangled photon rate. For entangled photon input rates on the order of

10^6 photons/s, the noise level is around 10^3 counts/s, which corresponds to 0.1 % of the input rate.

The error in the ETPA signal is measured by taking multiple measurements (in our experiment, 5) at each input rate. The standard deviations of the measured transmitted count rates for the solvent reference and the chromophore solution are propagated to calculate error bars. This error accounts for fluctuations in the input entangled photon rate, caused primarily by power fluctuations of the CW pump laser, and accounts for the electronic noise of the APDs and counter. For entangled photon input rates on the order of 10^6 photons/s, the typical error is around 10^3 counts/s, the same as the 0.1 % noise level. These results were summarized in Table 3 in the main manuscript.

ETPA with Collinear Type-I CW-Pumped SPDC

Results for the ETPA rate using collinear phase-matched Type-I degenerate, CW-pumped SPDC are shown in Fig. S4

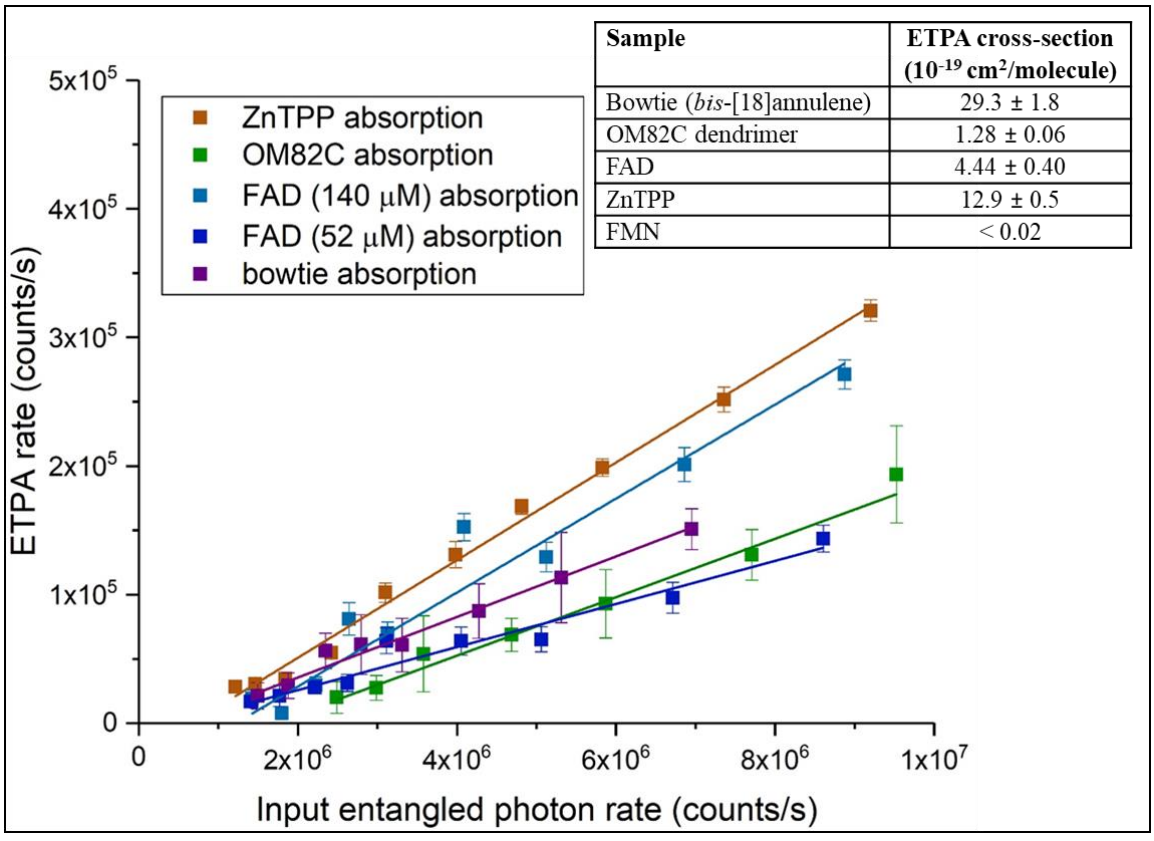

Sample	ETPA cross-section (10^{-19} cm^2/molecule)
Bowtie (*bis*-[18]annulene)	29.3 ± 1.8
OM82C dendrimer	1.28 ± 0.06
FAD	4.44 ± 0.40
ZnTPP	12.9 ± 0.5
FMN	< 0.02

Figure S4. ETPA results obtained with type-I collinear SPDC entangled photons excitation.

Fluorescence ETPA experiments.

For fluorescence ETPA experiments, the entangled photons were focused by using a plano-convex lens, *fl* = 2.5 cm. A previously designed fluorescence collection unit (Ref. [8] and references therein), λ_{cut} = 450 and 650 nm long and short pass filters, and a photomultiplier tube with a single photon counting module were used to isolate and detect the ETPA induced fluorescence signal.

4) ***Control on the population of a final state through the frequency joint spectrum***

The probability on a three-level system to be in a final state *f*, driven by entangled two-photon excitation from the ground state (*g*) and using intermediate states (*e*), as a function of time, obtained perturbatively is[9]:

$$\langle \hat{p}_f(t) \rangle_\psi = \langle \hat{T}_{fg}^\dagger(t) \hat{T}_{fg}(t) \rangle \tag{S2}$$

The transition amplitude corresponds to:

$$\hat{T}_{fg}(t) = \int d\omega_1 \int d\omega_2 \, T_t(\omega_1, \omega_2) \hat{E}_2(\omega_2) \hat{E}_1(\omega_1) \tag{S3}$$

$$T_t(\omega_1, \omega_2) = \left(\frac{E_0}{\hbar}\right)^2 \sum_e \left(\frac{\mu_{ge}}{\omega_1 - \omega_e + i\gamma_e} + \frac{\mu_{ge}}{\omega_2 - \omega_e + i\gamma_e}\right)\left(\frac{\mu_{ef}}{\omega_1 + \omega_2 - \omega_f + i\gamma_f} e^{-\boldsymbol{i}(\omega_1+\omega_2)t}\right) \tag{S4}$$

$\hat{T}_{fg}(t)$ is expressed in terms of the transition dipole moments (μ_{ge} and μ_{ef}) and subscripts 1 and 2 represent signal and/or idler photon. ω_e and ω_f correspond to the energy of the intermediate and final states; and γ_x ($x = e, f$) is the state linewidth.

As can be seen from equations (S2) – (S4), the population of a particular final excited state can be adjusted precisely by tuning the frequency correlations of the entangled pair.[9,10] The frequency correlation can be controlled by shaping the spatial distribution of the pump beam. It was demonstrated that the optimal T_f function can be represented in a Schmidt decomposition of the matter response function as[9]

$$T_t(\omega_1, \omega_2) = \sum_k r_k \psi_k^*(\omega_1) \, \phi_k^*(\omega_2) \tag{S5}$$

ψ_k and ϕ_k functions form an orthonormal basis set, with r_k chosen to be real and positive numbers. This orthonormal set is also a way to represent the ideal joint spectrum of the entangled

photon pairs inducing with maximum probability the ETPA transition from an initial to final states through selectively excited intermediate states.

References

(1) Fedorov, M. V.; Mikhailova, Y. M.; Volkov, P. A. Gaussian Modelling and Schmidt Modes of SPDC Biphoton States. *J. Phys. B: At. Mol. Opt. Phys.* **2009**, *42*, 175503.

(2) Villabona-Monsalve, J. P.; Calderón-Losada, O.; Nuñez Portela, M.; Valencia, A. Entangled Two Photon Absorption Cross Section on the 808 nm Region for the Common Dyes Zinc Tetraphenylporphyrin and Rhodamine B. *J. Phys. Chem. A* **2017**, *121*, 7869-7875.

(3) Anglister, J.; Steinberg, I. Z. Depolarized Rayleigh Light Scattering in Absorption Bands Measured in Lycopene Solution. *Chem. Phys. Lett.* **1979**, *65*, 50-54.

(4) Anglister, J.; Steinberg, I. Z. Resonance Rayleigh Scattering of Cyanine Dyes in Solution. *J. Chem. Phys.* **1983**, *78*, 5358-5368.

(5) Xu, C.; Shear, J. B.; Webb, W. W. Hyper-Rayleigh and Hyper-Raman Scattering Background of Liquid Water in Two-Photon Excited Fluorescence Detection. *Anal. Chem.* **1997**, *69*, 1285-1287.

(6) Wang, C.-K.; Macak, P.; Luo, Y.; Ågren, H. Effects of Π Centers and Symmetry on Two-Photon Absorption Cross Sections of Organic Chromophores. *J. Chem. Phys.* **2001**, *114*, 9813-9820.

(7) Schomacker, K. T.; Delaney, J. K.; Champion, P. M. Measurements of the Absolute Raman Cross-Sections of Benzene. *J. Chem. Phys.* **1986**, *85*, 4240-4247.

(8) Varnavski, O.; Pinsky, B.; Goodson, T. Entangled Photon Excited Fluorescence in Organic Materials: An Ultrafast Coincidence Detector. *J. Phys. Chem. Lett.* **2017**, *8*, 388-393.

(9) Schlawin, F.; Buchleitner, A. Theory of Coherent Control with Quantum Light. *New J. Phys.* **2017**, *19*, 013009.

(10) Roslyak, O.; Marx, C. A.; Mukamel, S. Nonlinear Spectroscopy with Entangled Photons: Manipulating Quantum Pathways of Matter. *Phys. Rev. A* **2009**, *79*, 033832.